# *Electronic Supplementary Information*

# **Significantly boosted oxygen electrocatalysis from the cooperation between cobalt and iron porphyrins**

Haitao Lei, Qingxin Zhang, Yabo Wang, Yimei Gao, Yanzhi Wang, Zuozhong Liang, Wei Zhang* and Rui Cao*

*Key Laboratory of Applied Surface and Colloid Chemistry, Ministry of Education, School of Chemistry and Chemical Engineering, Shaanxi Normal University, Xi'an 710119, China.*

*Correspondence E-mails: zw@snnu.edu.cn; ruicao@snnu.edu.cn

## 1. General methods and materials.

Materials that are sensitive to air and moisture were manipulated under argon using standard Schlenk line techniques. All reagents were commercially available and were used directly unless otherwise noted. Dry solvents, including dichloromethane, hexane, acetonitrile, and dimethylformamide were used in this work. All aqueous solutions were prepared freshly using the Milli-Q water. Multiwalled CNTs (>95% purity, <8 nm outside diameter, 3 nm inside diameter) were commercially available. High-resolution mass spectra were obtained using Brüker MAXIS. UV-vis spectra were measured using a Hitachi U-3310 spectrophotometer. $^1$H NMR spectroscopic measurements were acquired on a Brüker spectrometer operating at 400 MHz. Transmission electron microscopy (TEM) images were obtained using JEOL JEM-2100 with a 200 kV accelerating voltage. Hitachi SU8020 cold-emission field emission scanning electron microscope (FE-SEM) was used to study the sample morphologies with an accelerating voltage of 1 kV. Energy dispersive X-ray (EDX) spectra were measured from three areas of each sample to ensure the chemical homogeneity. X-ray photoelectron spectroscopy (XPS) data were collected by ESCALab 220i-XL electron spectrometer from VG Scientific using 300 W Al Kα radiation. The C 1s peak at 284.6 eV arising from adventitious hydrocarbon was used for the correction of binding energies. All samples used were carefully prepared via centrifugation and redispersion.

## 2. Synthesis.

*Synthesis of tetrakis(pentafluorophenyl)porphyrin*. To a round bottom flask equipped with a magnetic stirrer, pentafluorobenzaldehyde (1.45 g, 7.5 mmol) and pyrrole (0.5 g, 7.5 mmol) were dissolved in propionic acid (40 mL). The mixture was refluxed for 2.5 h, and was then dried using a rotary evaporator. The dark residue was dissolved in $CH_2Cl_2$, and was washed with saturated aqueous sodium carbonate and water, successively. The organic layer was separated and dried over anhydrous sodium sulfate and evaporated to dryness. The resulting residue was purified by silica-gel column chromatography (hexanes/$CH_2Cl_2$ = 10:1 v/v) to afford tetrakis(pentafluorophenyl)porphyrin as a purple solid (0.26 g, 14%). $^1$H NMR (400 MHz, CDCl$_3$): δ = 8.93 (s, 8H), −2.91 (s, 2H) (Fig. S1).

*Synthesis of **Co-P***. Complex **Co-P** was prepared by refluxing cobalt acetate tetrahydrate (0.37 g, 1.50 mmol) and tetrakis(pentafluorophenyl)porphyrin (0.29 g, 0.30 mmol) in dimethylformamidine (25 mL) for 4 h. The dark residue was obtained by removing the solvent with a rotary evaporator, and then purified through a silica-gel column with hexanes/$CH_2Cl_2$ (8:1 v/v) as the eluting solvent to afford pure **Co-P** as a dark red solid (0.23 g, 75%). High-resolution ESI-MS for $C_{44}H_8F_{20}CoN_4$: calcd. 1030.9762; found, 1030.9757 (Fig. S4).

*Synthesis of **Fe-P***. Complex **Fe-P** was prepared by refluxing iron dichloride (0.38 g, 3.00 mmol) and tetrakis(pentafluorophenyl)porphyrin (0.29 g, 0.30 mmol) in a mixture of

CHCl$_3$/EtOH (25 mL, 5:1 v/v) for 1 h. After rotary evaporator, the dark residue was redissolved in CH$_2$Cl$_2$ and washed with 2 M HCl, and then purified through a silica-gel column with CH$_2$Cl$_2$/MeOH (95:5 v/v) as the eluting solvent to afford pure **Fe-P** as a dark red solid (0.22 g, 68%). High-resolution ESI-MS for C$_{44}$H$_8$F$_{20}$FeN$_4$: calcd. 1027.9779; found, 1027.9769 (Fig. S5).

**3. Electrochemical Methods.**

Electrochemical measurements were carried out using CH Instruments (model CHI660D Electrochemical Analyzer). Cyclic voltammogram was collected in aqueous solutions using a three-compartment cell with a 0.071 cm$^2$ glassy carbon (GC) working electrode, graphite rod counter electrode, and Ag/AgCl (saturated KCl solution) reference electrode. Bipotentiostat (model DY2300 Electrochemical Analyzer) was used for rotating ring disk electrode measurements. The rotating disk electrode (RDE) has a GC disk electrode (0.071 cm$^2$, ALS RDE-2). The rotating ring-disk electrode (RRDE) has a GC disk electrode (0.125 cm$^2$) and a platinum ring electrode (0.188 cm$^2$, ALS RRDE-2). The collection efficiency of 0.425 was evaluated for this ring-disk electrode using the [Fe(CN)$_6$]$^{3-/4-}$ redox couple. In RRDE, the potential at GC disk electrode was scanned in the range of 0.1 to 1.0 V whereas the potential at the Pt ring electrode was held at 1.46 V to detect H$_2$O$_2$.

The $H_2O_2$ yield can be calculated according to current densities at the disk ($I_d$) and the ring ($I_r$) electrodes using the following equation:

$$\%H_2O_2 = 200 \times \frac{\frac{I_r}{N}}{I_d + \frac{I_r}{N}}$$

in which $N = 0.425$ is the current collection efficiency of the Pt ring.

In addition, the number of electrons ($n$) transferred per $O_2$ molecule could be calculated using the Koutecky-Levich (K-L) analysis in rotating disk electrode measurements using the equation:

$$\frac{1}{j} = \frac{1}{j_k} + \frac{1}{j_d} = -\frac{1}{nFkC_{O_2}} - \frac{1}{0.2nFD_{O_2}^{2/3}v^{-1/6}C_{O_2}\omega^{1/2}}$$

in which $j$ is the measured current density, $j_k$ and $j_d$ are the kinetic and diffusion-limited current densities, respectively, $n$ is the number of electrons transferred per molecule of $O_2$, $F$ is the Faraday constant (96485 C mol$^{-1}$), $k$ is the rate constant for ORR, $C_{O_2}$ is the concentration of $O_2$ dissolved in the bulk solution ($1.3 \times 10^{-6}$ mol cm$^{-3}$), $D_{O_2}$ is the diffusion coefficient of $O_2$ ($1.7 \times 10^{-5}$ cm$^2$ s$^{-1}$), $v$ is the kinematic viscosity of the solution (0.01 cm$^2$ s$^{-1}$), and $\omega$ (rpm) is the rotation rate. The constant 0.2 is adopted when the rotation speed is expressed in rpm.

The OER tests were carried out on a DY2300 Electrochemical Analyzer electrochemical workstation at room temperature. The OER performances were tested using a three-electrode system. The working electrode was a rotating disk electrode has a

GC disk electrode (0.071 cm$^2$, ALS RDE-2). The counter electrode was a graphitic rod. The reference electrode was saturated Ag/AgCl electrode. The linear sweep voltammetry (LSV) tests were carried out in 0.1 M KOH (scan rate of 5 mV s$^{-1}$).

## 4. Preparation of catalyst-loaded electrodes.

Generally, 1.0 mg of metal porphyrin and 1.0 mg of CNT were added to 1.0 mL of 6:1:3 v/v/v acetonitrile/dimethylformamide/isopropyl alcohol mixed solvent with 30 μL of Nafion solution (5 wt %, Dupont). The mixture was then ultrasonicated for about 0.5 h to generate a homogeneous ink (2 mg/mL). Next, the homogeneous suspension was added onto a GC electrode (6 μL), RDE disk electrode (6 μL) or RRDE disk electrode (10 μL) using a pipet. The electrodes were then dried slowly under dark.

## 5. Zn-air battery.

The anode was prepared using a polished Zn foil (0.25 mm). The air electrode was prepared using (**Co-P**)$_{0.5}$(**Fe-P**)$_{0.5}$@CNT or Pt/C coated carbon cloth (CC)/gas diffusion layer (GDL). A hot-press method was used to attach the CC (1.5 × 1.5 cm$^2$) onto the GDL. A catalyst loading of 2 mg cm$^{-2}$ on the CC/GDL was obtained. The electrolyte was an aqueous solution with 0.2 M ZnCl$_2$ and 6.0 M KOH.
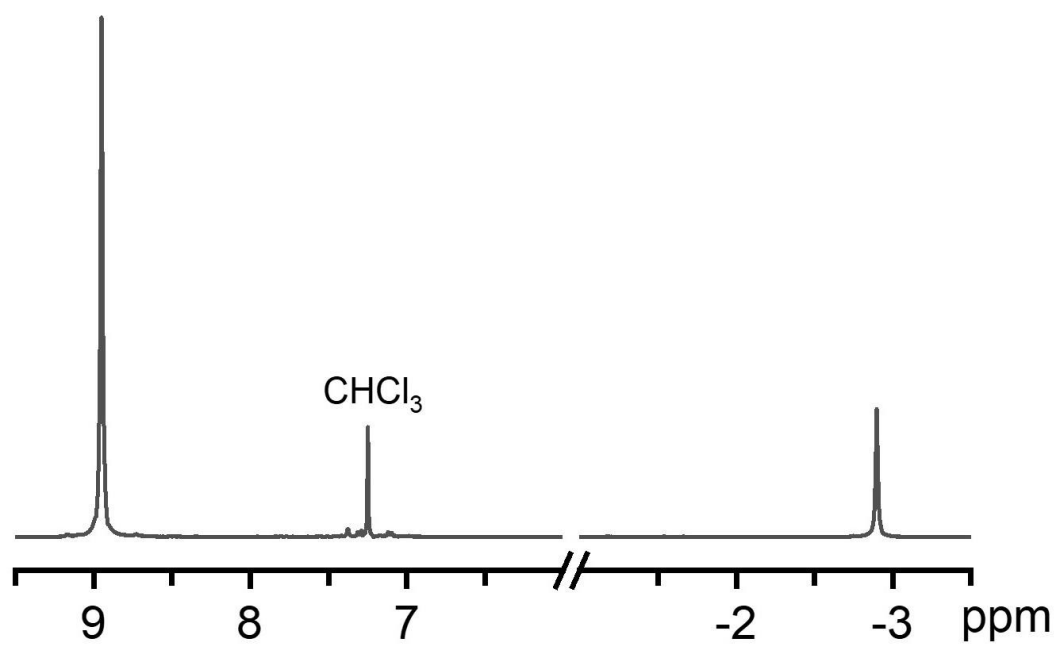
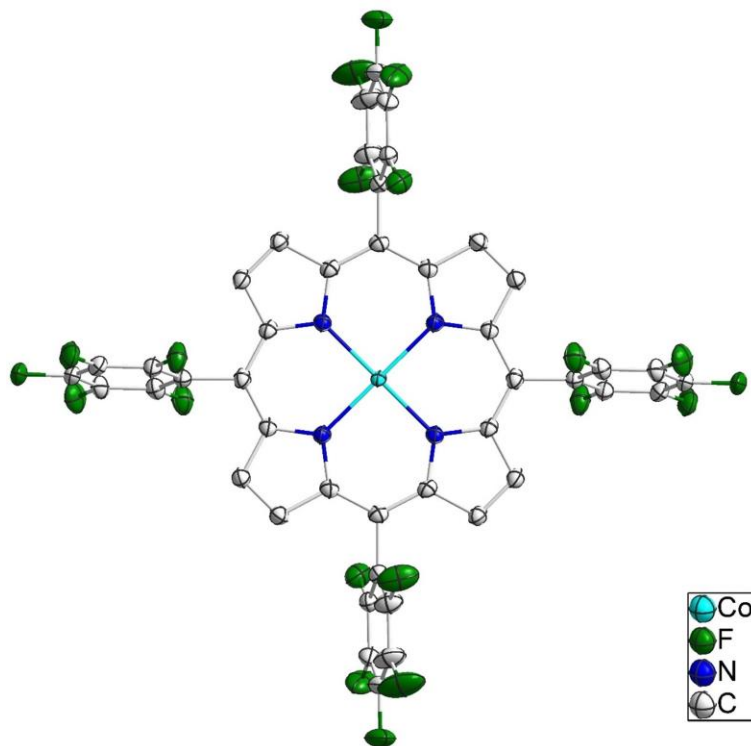**Fig. S1** $^{1}$H NMR spectrum of tetrakis(pentafluorophenyl)porphyrin.

**Fig. S2** Thermal ellipsoid plot (50% probability) of the X-ray structures of **Co-P**.

Hydrogen atoms and co-crystallized solvent molecules are omitted for clarity.
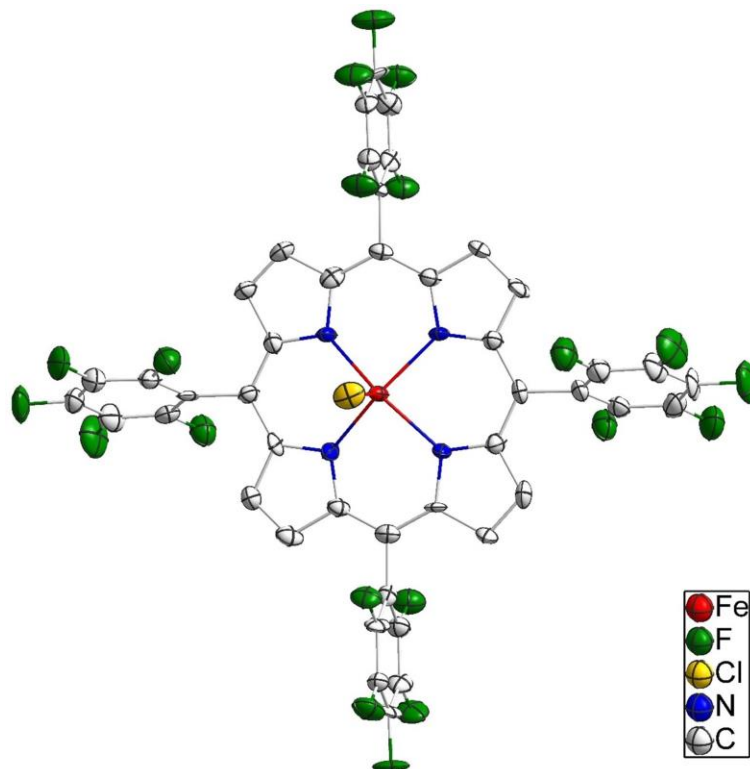
**Fig. S3** Thermal ellipsoid plot (50% probability) of the X-ray structures of **Fe-P**. Hydrogen atoms and co-crystallized solvent molecules are omitted for clarity.
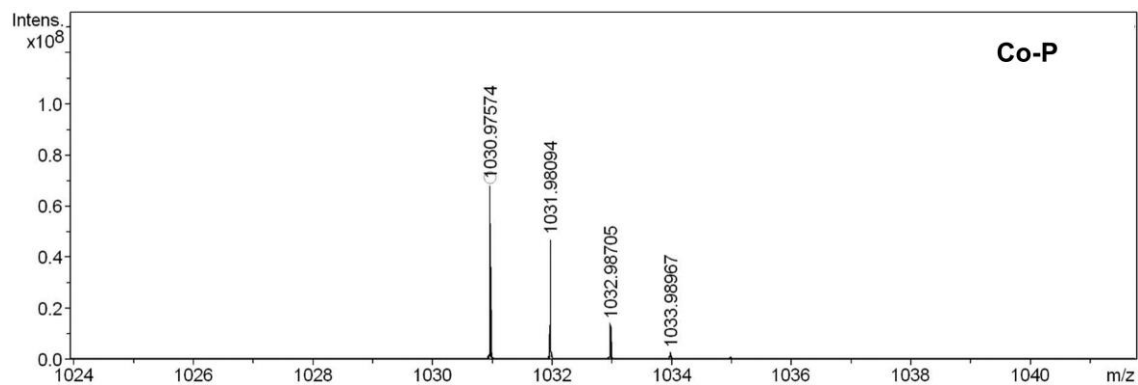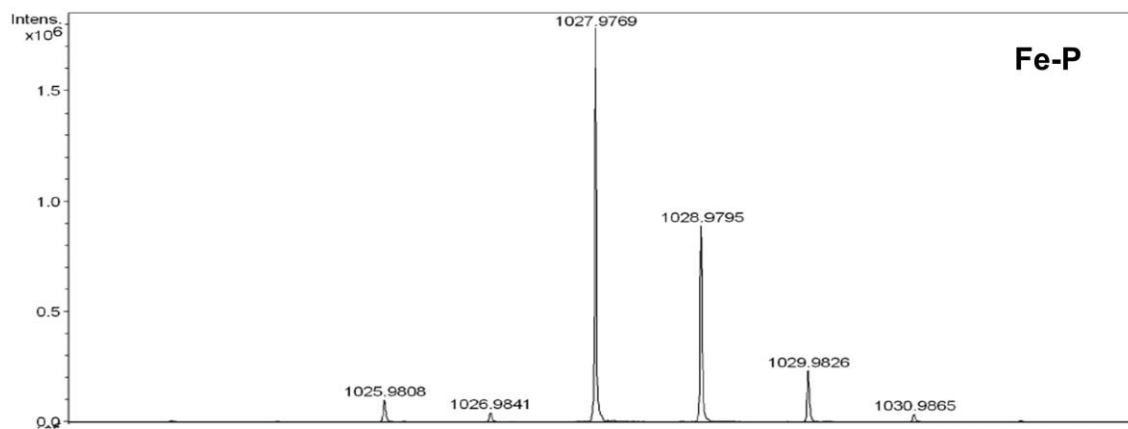
**Fig. S4** High-resolution mass spectrum of **Co-P** in methanol, showing a peak at 1030.9757, which corresponds to $C_{44}H_8F_{20}CoN_4$. This value is consistent with the calculated number of 1030.9762 for **Co-P**.

**Fig. S5** High-resolution mass spectrum of **Fe-P** in methanol, showing a peak at 1027.9769, which corresponds to $C_{44}H_8F_{20}FeN_4$. This value is consistent with the calculated number of 1027.9779 for $[\text{Fe-P} - Cl]^+$.
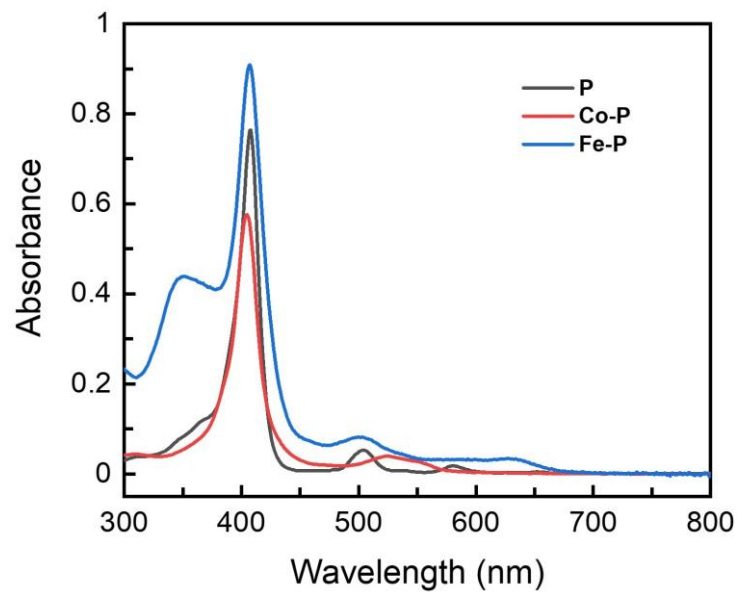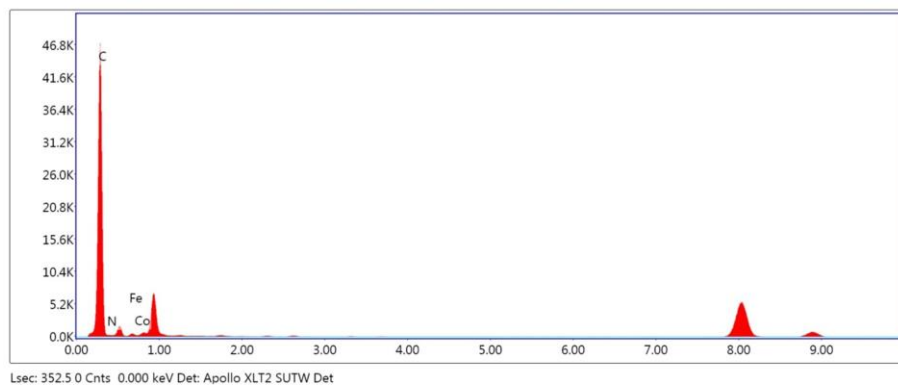
**Fig. S6** UV-vis spectra of tetrakis(pentafluorophenyl)porphyrin (**P**), **Co-P** and **Fe-P** in acetonitrile.

Lsec: 352.5 0 Cnts  0.000 keV Det: Apollo XLT2 SUTW Det

| Element | Weight % | Atomic % | Net Int. | Net Error% | KABFactor |
|---------|----------|----------|----------|------------|-----------|
| C K | 97.03 | 98.02 | 139.5 | 0.50 | 1 |
| N K | 2.07 | 1.79 | 2.8 | 4.38 | 1.08 |
| FeK | 0.37 | 0.08 | 0.6 | 37.37 | 0.89 |
| CoK | 0.53 | 0.10 | 0.8 | 8.93 | 0.94 |

**Fig. S7** EDX of $(\mathbf{Co\text{-}P})_{0.5}(\mathbf{Fe\text{-}P})_{0.5}$@CNT. The atom ratio of Fe and Co is 0.08:0.10.

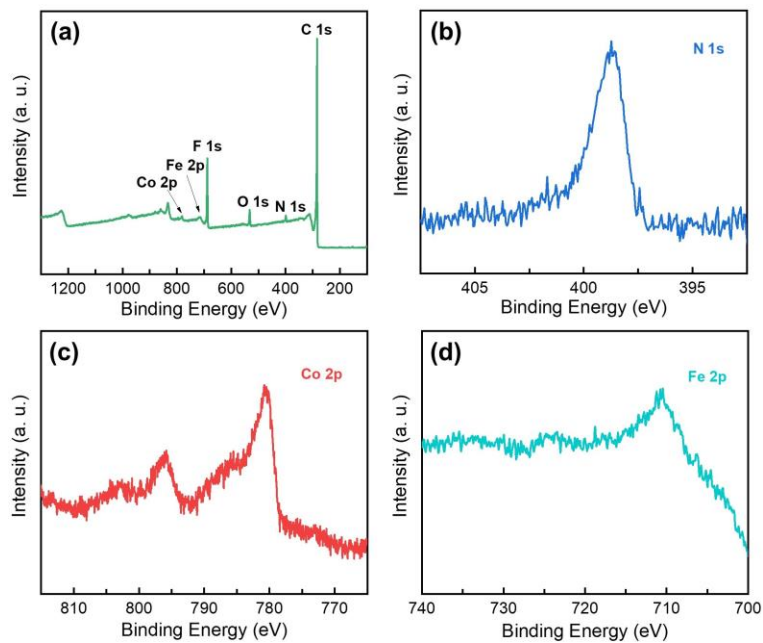**Fig. S8** (a) XPS survey spectra of (**Co-P**)$_{0.5}$(**Fe-P**)$_{0.5}$@CNT. High-resolution XPS narrow scan spectra of N 1s (b), Co 2p (c) and Fe 2p (d) of (**Co-P**)$_{0.5}$(**Fe-P**)$_{0.5}$@CNT.
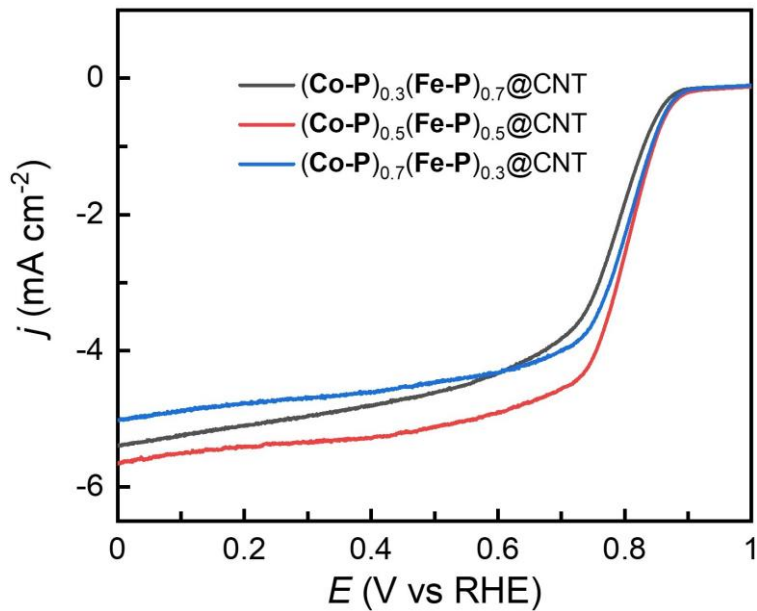
**Fig. S9** RDE data of $(\textbf{Co-P})_{0.3}(\textbf{Fe-P})_{0.7}$@CNT, $(\textbf{Co-P})_{0.5}(\textbf{Fe-P})_{0.5}$@CNT and $(\textbf{Co-P})_{0.7}(\textbf{Fe-P})_{0.3}$@CNT in 0.1 M KOH solution at 1600 rpm rotation rate.
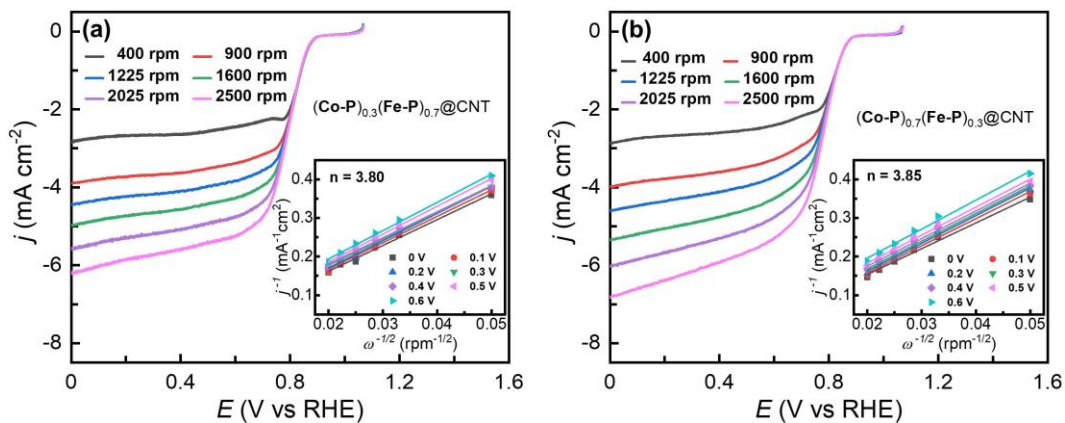
**Fig. S10** RDE data of $(\text{Co-P})_{0.3}(\text{Fe-P})_{0.7}$@CNT (a) and $(\text{Co-P})_{0.7}(\text{Fe-P})_{0.3}$@CNT (b) at different rotation rates. Inset: K-L plot of $j^{-1}$ versus $\omega^{-1}$.
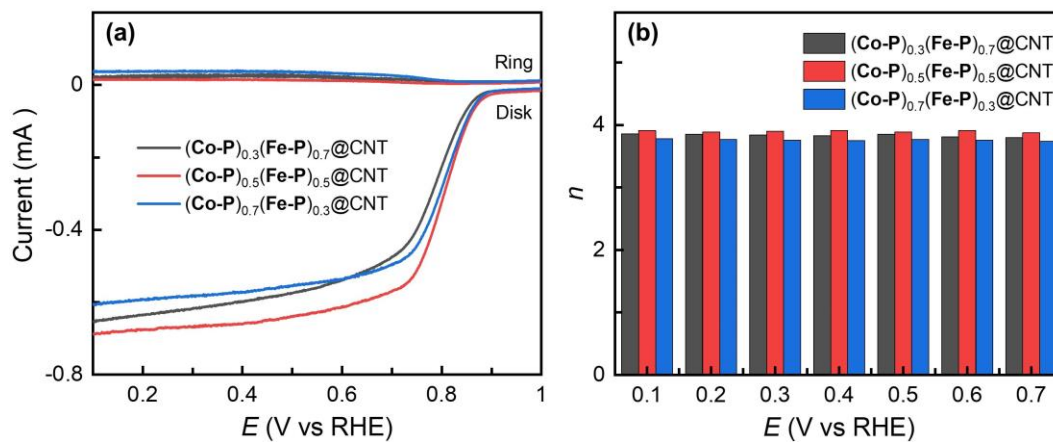
**Fig. S11** (a) RRDE measurements for $O_2$ reduction at the GC disk electrode with the samples in an $O_2$-saturated 0.1 M KOH solution at 1600 rpm. (b) $n$ value of $O_2$ reduction with the samples.
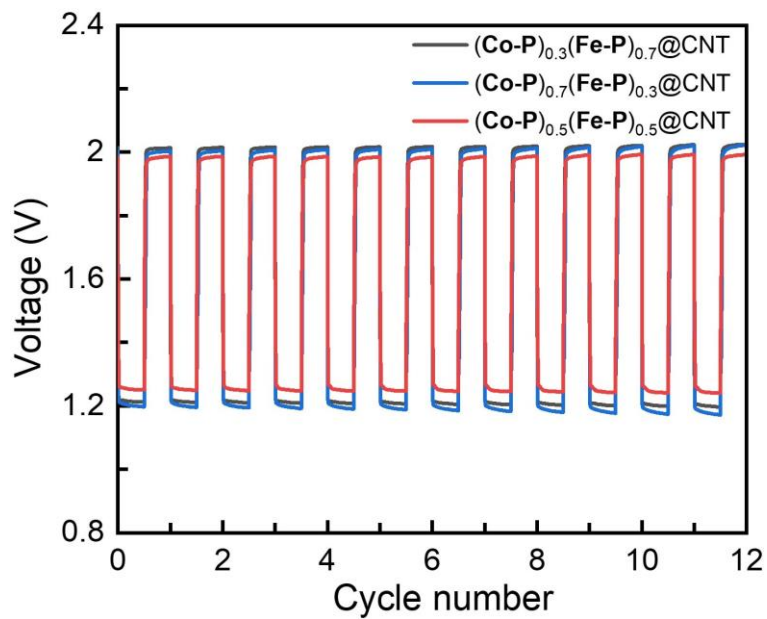
**Fig. S12** Galvanostatic discharge-charge cycling data at 2 mA cm$^{-2}$ of **(Co-P)**$_{0.3}$**(Fe-P)**$_{0.7}$@CNT, **(Co-P)**$_{0.5}$**(Fe-P)**$_{0.5}$@CNT and **(Co-P)**$_{0.7}$**(Fe-P)**$_{0.3}$@CNT.

**Table S1.** Metal contents of $(Co-P)_{0.3}(Fe-P)_{0.7}@CNT$, $(Co-P)_{0.5}(Fe-P)_{0.5}@CNT$ and $(Co-P)_{0.7}(Fe-P)_{0.3}@CNT$ as determined by ICP-MS.

| Sample | $(Co-P)_{0.3}(Fe-P)_{0.7}@CNT$ | $(Co-P)_{0.5}(Fe-P)_{0.5}@CNT$ | $(Co-P)_{0.7}(Fe-P)_{0.3}@CNT$ |
|---|---|---|---|
| Co content (µg/mg hybrid) | 7.71 | 12.85 | 17.91 |
| Fe content (µg/mg hybrid) | 16.53 | 11.81 | 7.08 |

**Table S2.** Comparison of ORR metal porphyrin electrocatalysts.

| Catalyst | Half-wave potential | $n$ | Ref. |
|---|---|---|---|
| (**Co-P**)$_{0.5}$(**Fe-P**)$_{0.5}$@CNT | 0.80 | 3.98 | ***This work*** |
| Co(C$_6$F$_5$)$_4$/CNTs | 0.45 V | 2.90 | *Chem. Sci.* 2010, *1*, 411-414 |
| (TPP)Co/EPPG | 0.39 V | 2.00 | *Inorg. Chem.* 2017, *56*, 13613-13626 |
| CoEtP/CNTs | 0.77 V | 2.44 | *Carbon* 2011, *49*, 4839-4847 |
| GCCo | 0.71 V | 2.00 | *Int. J. Electrochem. Sci.* 2018, *13*, 1666-1682 |
| CPCo-1@C | 0.45 V | 2.24 | *ACS Appl. Mater. Interfaces* 2020, *12*, 45976-45986 |
| MWNT-1Fe | 0.66 V | 3.97 | *J. Porphyrins Phthalocyanines* 2020, *24*, 681-684 |
| MWNT–FeP | 0.54 V | 3.96 | *New J. Chem.* 2018, *42*, 19749-19754 |
| GCCo-Fe 1:1 | 0.79 V | 4.2 | *Int. J. Electrochem. Sci.* 2018, *13*, 1666-1682 |